Dielectric Dispersion of Polypeptide Solutions. II. Helix–Coil Transition of Poly(ε-carbobenzoxy-L-lysine) in *m*-Cresol

Ikuo Omura, Akio Teramoto,* and Hiroshi Fujita

Department of Polymer Science, Osaka University, Osaka 560, Japan.
Received September 20, 1974

ABSTRACT: Dielectric dispersion measurements were made on dilute solutions of poly(ε-carbobenzoxy-L-lysine) in *m*-cresol; this system underwent a very sharp thermal helix–coil transition of inverse type around 30°. Mean-square dipole moments $\langle\mu^2\rangle$ and mean rotational relaxation times τ were obtained as functions of molecular weight and helical fraction f_N. It was found that $\langle\mu^2\rangle^{1/2}$ varied almost linearly with $f_N^{1/2}$ over a substantial portion of the transition. The relaxation times corrected for solvent viscosity and temperature changed only slightly with f_N except in the region of small f_N, while, at fixed f_N, they displayed molecular weight dependence characteristic of rod-like molecules. These results can be explained if the transition is assumed to proceed almost in all-or-none fashion. This assumption is consistent with the previous finding from statistical thermodynamic analyses that the transition of the system PCBL–*m*-cresol is highly cooperative, with $\sigma^{1/2}$ being 0.0025 to 0.0027, where σ is the cooperativity parameter. Application of Nagai's theory of $\langle\mu^2\rangle$ for interrupted helices yielded the result that $\sigma^{1/2}$ was in the range 0.001 to 0.005 and the monomeric dipole moment in the helical conformation was 5.4 to 6.2 D.

The present paper reports a study of the system poly(ε-carbobenzoxy-L-lysine)(PCBL)–*m*-cresol in the helix–coil transition region by dielectric dispersion measurements. This system was chosen because recent thermodynamic analyses had revealed an unusually strong cooperativity for the helix formation of PCBL in *m*-cresol.[1,2a] In fact, the cooperativity parameter σ was smaller by a factor of about 10 or more than those reported for many other polypeptides such as poly(γ-benzyl L-glutamate) (PBLG)[3-9] and poly(β-benzyl L-aspartate) (PBLA).[10,11] The transition of PCBL was found to be strongly cooperative also in dichloroacetic acid–ethylene dichloride mixtures.[1,2b] The principal purpose here is to explore characteristic changes which are expected to appear in $\langle\mu^2\rangle$ and τ when a system of such strong cooperativity undergoes a thermal helix–coil transition. Here $\langle\mu^2\rangle$ and τ denote the mean-square dipole moment and mean rotational relaxation time of the polypeptide, respectively.

One of the striking features of helix–coil transitions in polypeptides is that the transition process depends on the chain length of the polymer. Thus another purpose of the present study is to examine effects of this dependence on both $\langle\mu^2\rangle$ and τ as functions of helical fraction. Wada et al.[12] used the dielectric method to detect the helix–coil transitions of PBLA in *m*-cresol, and Marchal and colleagues[13-16] investigated the dielectric behavior of PBLG in solvent mixtures containing dichloroacetic acid (DCA). None of these reports provide information sufficient for our purposes stated above.

I. Experimental Section

The ε,*N*-carbobenzoxy-L-lysine-*N*-carboxy anhydride (NCA) prepared from ε,*N*-carbobenzoxy-L-lysine according to Fasman et al.[17] was first polymerized in dimethylformamide (DMF) with *n*-butylamine as initiator at the mole ratio of NCA to initiator fixed to 20. Then, an aliquot of this polymerization mixture was used to initiate polymerization of NCA dissolved in a dioxane–DMF mixture, with the NCA concentration and its ratio to initiator adjusted to the desired values. The resulting mixtures were poured into a large volume of 2-propanol, and the precipitated polymers were freeze dried from dioxane solutions. The PCBL samples so obtained had relatively narrow distributions in molecular weight as will be shown below, and were not subjected to further fractionation. Weight-average molecular weights of the samples were determined by the sedimentation equilibrium method.[1,18] Relevant data on these samples, together with those of two fractionated samples selected from our stock,[1] are summarized in Table I.

m-Cresol was distilled under dry nitrogen atmosphere (bp 61° (2 mm)). Dichloromethane (DCM, bp 40.4°) and ethylene dichloride (EDC, bp 83.5°) were dried and fractionally distilled over calcium hydride. Pure *m*-cresol and its mixtures with DCM or EDC were used as solvents in physical measurements. Solvent compositions and polymer concentrations were determined gravimetrically. Necessary data for densities and viscosities of *m*-cresol were taken from the literature,[19] while those of the mixed solvents were determined directly.

Dielectric measurements and optical rotation measurements were performed by the techniques as described in our previous papers.[1,20]

II. Results

A. Data in *m*-Cresol. 1. Optical Rotation. Figure 1 shows optical rotation data for PCBL in *m*-cresol, where the mean residue rotation for the wavelength 436 nm, $[m']_{436}$, is plotted against temperature. The ordinate on the right-hand side gives approximate values for helical fraction f_N computed by an empirical relation.[21] It is observed that this polypeptide in *m*-cresol undergoes an inverse thermal helix–coil transition. The transition is extremely sharp for higher molecular weight samples, but it becomes gentle and shifts to higher temperatures as the weight-average degree of polymerization $\bar{N}_w$ is decreased. These results supplement the recent data of Matsuoka et al.[1] for higher molecular weight samples. For sample L-652, $[m']_{436}$ approaches a plateau above 30°, which appears to indicate that the molecule becomes completely helical at such temperatures. Detailed examination in terms of the Moffitt–Yang parameter b_0 revealed, however, that f_N reaches a broad maximum in the range 30–50° for this and other higher molecular weight samples. The same trend was observed by Matsuoka et al.[1] for PCBL sample L-22 of very high molecular weight ($\bar{M}_w = 87 \times 10^4$). They also observed that the intrinsic viscosity $[\eta]$ of L-22 displayed a maximum in the same temperature range, but that the maximum was considerably lower than the $[\eta]$ in a helicogenic solvent DMF at 25°. From these we must conclude that the maximum helical fractions attained by high molecular weight PCBL in *m*-cresol at higher temperatures were still smaller than unity.

Attempts to determine the parameters s and σ in the theory of Zimm and Bragg[22] of helix–coil transition from the analysis of the $[m']_{436}$ and b_0 data below 35° were successful, giving similar results to those reported by Matsuoka et al.[1] Such analysis with the data above 35° was unsuccessful, since the experimental f_N–N relations did not

Table I
Molecular Weights of the PCBL Samples Studied

Sample code	$\bar{M}_w$	$\bar{N}_w$	$A_2 \times 10^4$, (ml mol)/g^2
L-651	134,000	511	4.3
L-652	87,000	332	6.2
M-1	47,200	180	4.0
M-2	30,700	117	4.9
M-3	39,000[a]		
M-4	23,400	89	5.3

[a] Determined from the intrinsic viscosity in *m*-cresol at 15°.[1]

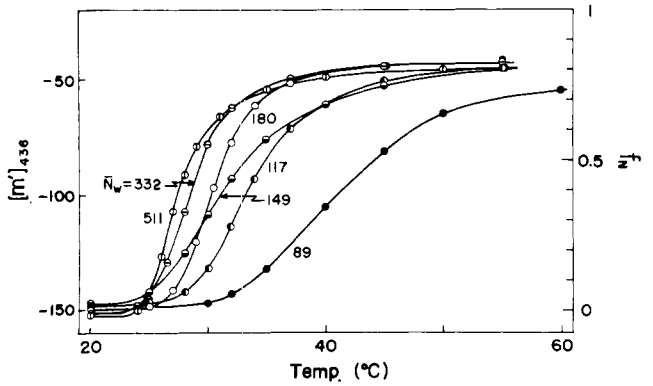

Figure 1. Optical rotation data for poly(ϵ-carbobenzoxy-L-lysine) (PCBL) in *m*-cresol. The ordinate on the right-hand side gives helical fraction f_N estimated from $[m']_{436}$.[21]

conform precisely to the theoretical prediction; it gave σ values increasing appreciably with raising temperature. On the other hand, usual analyses based on constant σ and transition enthalpy predicted consistently higher f_N values than the observed ones; the trend was more conspicuous at higher temperatures. However, it was found that almost constant values of σ could be obtained over the entire range of temperature studied if f_N were recalculated by adjusting b_0 for perfect helix to about −500 from −550 employed by Matsuoka et al.[1] Although at present no positive evidence is available to justify such adjustment, we assume that $\sigma^{1/2}$ for the PCBL–*m*-cresol system does not depend on temperature and assign to it either 0.0025 from the optical rotation measurements[1] or 0.0027 from the heat capacity measurements,[2a] both of which refer to about 25°.

2. Dielectric Dispersion. Figure 2 shows plots of conductance increment G vs. log f (f = frequency in hertz) for a *m*-cresol solution of sample M-2 at various temperatures. The curve for each temperature exhibits a single dispersion around 30 kHz and levels down to a constant value below 10 kHz. This constant value of G has been taken as that for dc conductance and subtracted from the observed G to compute the dielectric loss factor $\Delta\epsilon''$. The frequency dependence of $\Delta\epsilon''$ thus calculated is given in Figure 3, which displays a well-defined maximum at each temperature investigated. Figure 4 depicts plots of the corresponding dielectric increment $\Delta\epsilon'$ vs. log f. Each curve also exhibits a dispersion region which is located around 30 kHz, conforming to the dielectric loss factor data given above. However, at low frequencies, it does not approach a well-defined plateau region, but rises first gradually and then sharply as f is decreased. This phenomenon may be attributed to the polarization near electrode surfaces due to the possible contamination of the polypeptide samples.

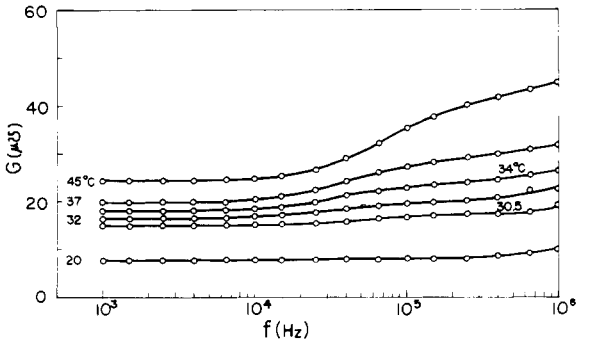

Figure 2. Conductance increments G plotted vs. log f for PCBL M-2 in *m*-cresol at the indicated temperatures. The polymer concentration was 4.42×10^{-3} g/ml at 45°.

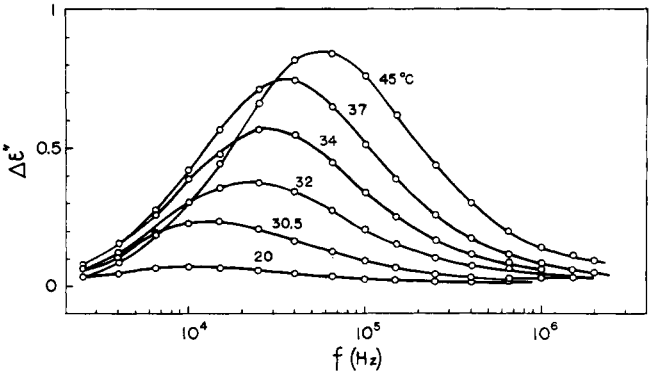

Figure 3. Plots of dielectric loss factor $\Delta\epsilon''$ vs. log f for PCBL M-2 in *m*-cresol at the indicated temperatures.

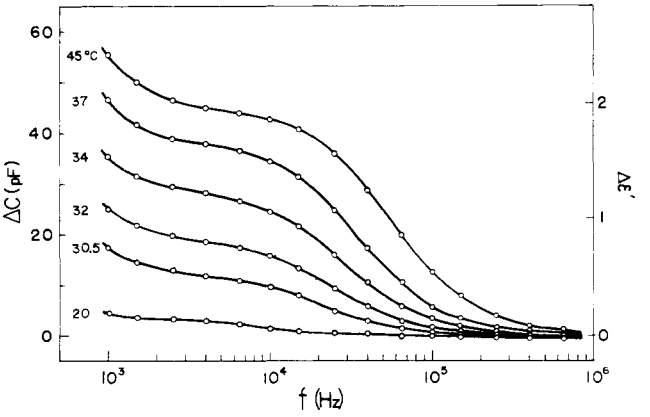

Figure 4. Plots of dielectric increment $\Delta\epsilon'$ vs. log f for PCBL M-2 in *m*-cresol.

Figure 5 shows Cole–Cole arc plots for sample M-2 constructed from the data given in Figures 3 and 4. The data points at each temperature form a semicircle with its center located close to the $\Delta\epsilon'$ axis. These results suggest that the distribution of rotational relaxation times is relatively narrow at any stage of the transition from random coil to helix. The segment cut out of the $\Delta\epsilon'$ axis by the arc is taken to be the static dielectric increment $\Delta\epsilon$, and the frequency f_c corresponding to the summit of the arc is related to the mean rotational relaxation time τ by $\tau = 1/(2\pi f_c)$.

3. Mean-Square Dipole Moment. It can be seen from Figure 5 that PCBL molecules in the helical state have much greater contribution to the orientation polarization than those in the random coil state. This is expected because, in the helical state, dipoles of backbone peptide residues are arranged approximately parallel to the helix axis

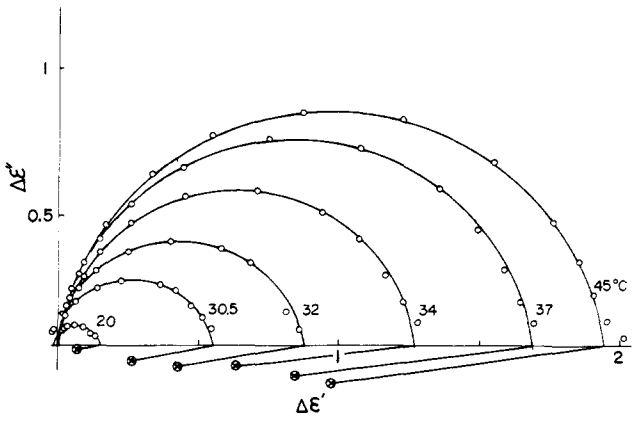

Figure 5. Cole–Cole plots for PCBL M-2 in *m*-cresol constructed from the data given in Figures 3 and 4. $f_N = 0.75_7$ at 45°, 0.59_0 at 37°, 0.42_6 at 34°, 0.27_4 at 32°, 0.17_6 at 30.5°, and 0.04 at 20°.

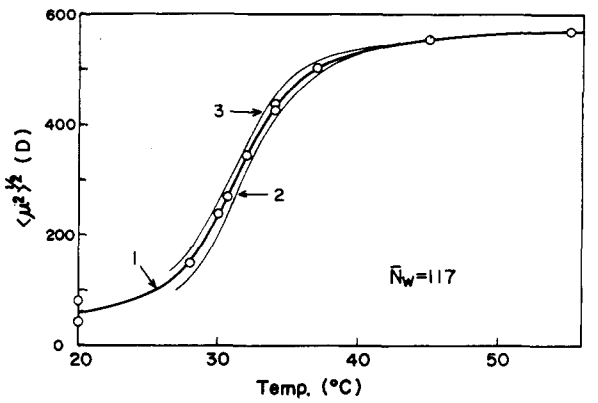

Figure 6. Temperature dependence of $\langle\mu^2\rangle^{1/2}$ for PCBL M-2 in *m*-cresol: curve 1, $\langle\mu^2\rangle^{1/2}$ computed by use of eq 2; curve 2, $\langle\mu^2\rangle^{1/2}$ computed by use of eq 3; curve 3, $\langle\mu^2\rangle^{1/2}$ computed by assuming $p = \bar{N}_w/10$ (see text).

to form a giant permanent dipole, whereas no such arrangement exists in the random coil state. For a quantitative discussion of molecular conformation in terms of dielectric data, the "vacuum" dipole moment $\langle\mu^2\rangle^{1/2}$ must be used, but at present we have no rigorous theory which allows $\langle\mu^2\rangle$ of a molecule of arbitrary shape embedded in a polar medium to be evaluated from experimentally measured $\Delta\epsilon$. The usual approximate procedure for synthetic polypeptides in helicogenic solvents is to utilize Wada's equation[12,23] or Buckingham's equation[24] modified by Applequist and Mahr.[25] For dilute solutions these equations can be summarized in the form[20]

$$\langle\mu^2\rangle = \frac{3kTM}{4\pi N_A}(\Delta\epsilon/c)(q/fg) \qquad (1)$$

where M is the molecular weight of the solute, k is the Boltzmann constant, T is the absolute temperature, N_A is the Avogadro number, and c is the solute concentration expressed in grams per milliliter. The factor q/fg is unity in Wada's equation, whereas it depends on the shape of the solute molecule in Buckingham's equation. From a theoretical point of view, Buckingham's equation may be more appropriate than Wada's for rodlike molecules, because it takes explicitly the molecular asymmetry into account.

For its application we need the axial ratio p of the molecule. However, we have no justifiable way to evaluate p of a partially helical polypeptide. Hence we resort to the following approximation. Buckingham's theory applies to a uniformly polarized ellipsoid of revolution embedded in a

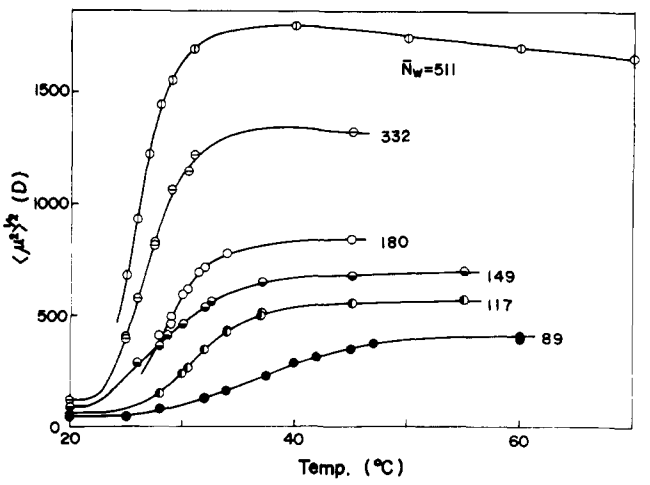

Figure 7. Temperature dependence of $\langle\mu^2\rangle^{1/2}$ for PCBL in *m*-cresol. The $\bar{N}_w$ of each sample is indicated on the figure.

continuum; this ellipsoid is actually the cavity formed by the dipolar solute itself. For random coils, the distribution of dipoles in the cavity should be symmetric, so that we may set $p = 1$. For perfectly helical polypeptides, the shape of the cavity may be approximated by an elongated ellipsoid of revolution with the major axis equal to the helix length and the minor axis of 15 Å. This yields $p = \bar{N}_w/10$. Hence, for partial helices the following interpolation formulas may be invoked.

$$p = 1 + [(\bar{N}_w/10) - 1]f_N^{1/2} \qquad (2)$$

$$p = 1 + [(\bar{N}_w/10) - 1]f_N \qquad (3)$$

In Figure 6, the values for $\langle\mu^2\rangle^{1/2}$ calculated by eq 2 (curve 1) are compared with those obtained by eq 3 (curve 2) and those obtained by assuming $p = \bar{N}_w/10$ irrespective of f_N (curve 3). The difference among these three curves becomes significant only at low temperatures where the molecular conformation approaches random coils. In the subsequent discussion we use eq 2 for the reason which is justified in subsection B of the Discussion section.

Figure 7 summarizes $\langle\mu^2\rangle^{1/2}$ so computed for all the PCBL samples studied, which range in $\bar{N}_w$ from 89 to 511. Similarity of this system of curves to the transition curves in Figure 1 indicates that the molecular dimensions of PCBL expand rapidly as the helical fraction increases, because the mean-square dipole moment is an analog of the mean-square end-to-end distance $\langle R^2\rangle$ for a linear chain molecule. Comparison of Figures 1 and 7 shows that the rise of $\langle\mu^2\rangle^{1/2}$ with temperature occurs in advance of that of helical fraction. This feature is characteristic of the system PCBL–*m*-cresol, because the results calculated by other equations also exhibit a similar behavior. Recently, Marchal et al.[15] observed for PBLG in mixtures of inert solvents and DCA that the relative positions of dielectric and ORD transition curves on the temperature axis depended on the inert solvent used. Figure 8, in which $\langle\mu^2\rangle^{1/2}$ appears plotted against f_N, shows that $\langle\mu^2\rangle^{1/2}$ starts from a small but finite value at $f_N = 0$ and increases more rapidly than f_N. Interestingly, the dependence is almost linear in $f_N^{1/2}$.

4. Mean Rotational Relaxation Time. Figure 9 depicts plots of mean rotational relaxation time τ corrected for solvent viscosity η_0 and absolute temperature T against f_N. The striking feature is that except for the region of low f_N, $\tau T/\eta_0$ is almost constant. It is also noted that $\tau T/\eta_0$ at fixed f_N display pronounced molecular weight dependence. These are sharply contrasted with the results reported for

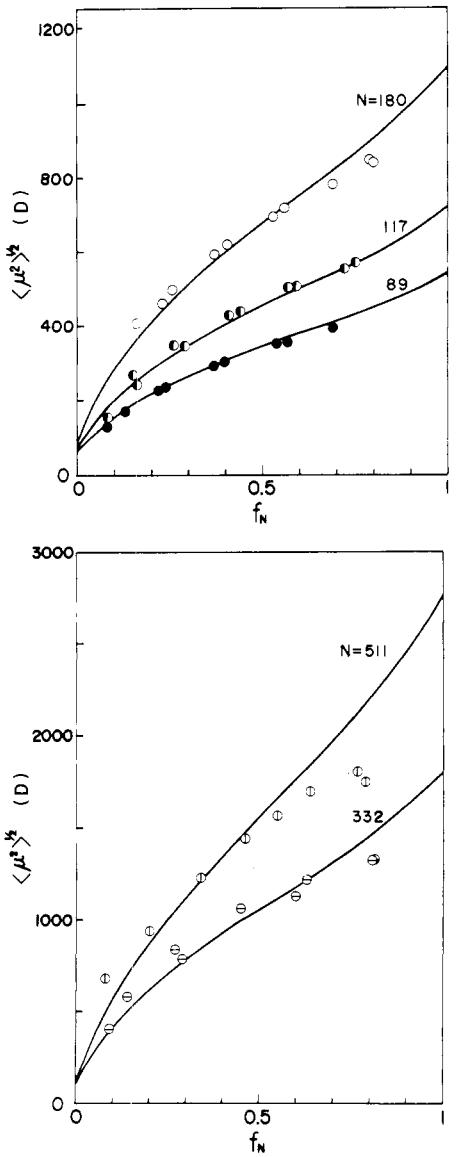

Figure 8. Plots of $\langle\mu^2\rangle^{1/2}$ vs. f_N for PCBL in *m*-cresol. (top) The data for the samples having $\bar{N}_w$: 180 (○), 117 (◐), 89 (●). The solid lines represent the theoretical values calculated with $\sigma^{1/2} = 0.0027$ and the assumption that $\mu_h = \mu_c = 6.2$ D. (bottom) The data for L-651 ($\bar{N}_w = 511$) and L-652 ($\bar{N}_w = 332$). The solid lines represent the theoretical values calculated with $\sigma^{1/2} = 0.0027$ and the assumption that $\mu_c = \mu_h = 5.4$ D.

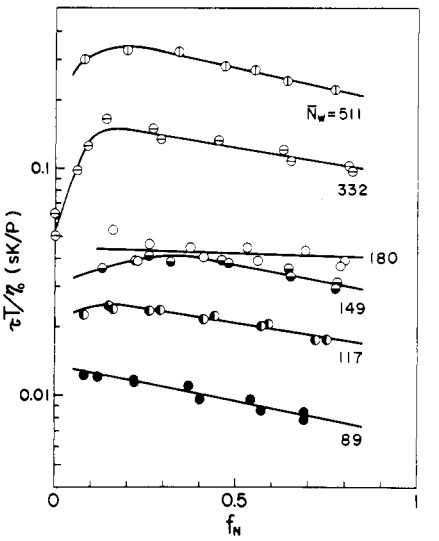

Figure 9. Mean rotational relaxation times as a function of helical fraction f_N for PCBL in *m*-cresol: $\tau T/\eta_0$ is given in units of sec deg/P.

Table II
Dielectric Data for PCBL under Helicogenic Conditions[d]

Sample code	Solvent	Temp, °C	$\langle\mu^2\rangle^{1/2}$, D	$\tau T/\eta_0 \times 10^2$, (sec deg)/P	f_N[a]	α[b]
M-4	*m*-Cresol	60	395	0.81	0.69	0.08
M-2	*m*-Cresol	45, 55	562	1.7	0.73	0.09
	EDC–*m*-cresol	20	620	1.9	0.91	0.08
M-3	*m*-Cresol	45, 55	687	3.0	0.78	0.17
M-1	*m*-Cresol	45	842	3.8	0.80	0.07
	EDC–*m*-cresol	30	923	4.0		0.06
	DCM–*m*-cresol	20	935	4.3		0.07
L-652	*m*-Cresol	45	1330	9.8		0.15
L-651	*m*-Cresol	40	1800	22	0.77	0.18
	EDC–*m*-cresol	30	1820	23	0.88	0.17
A-43[c]	*m*-Cresol	10				0.03
A-6[c]	*m*-Cresol	25				0.12
A-IV[c]	*m*-Cresol	25				0.22

[a] Calculated from b_0 by $f_N = (182 - b_0)/712$. [b] Cole–Cole's representation.[28] $\alpha = 0$ corresponds to monodisperse systems. [c] Data for PBLG taken from Matsumoto et al.[20] [d] The ratios $\bar{M}_w/\bar{M}_n$ are 1.27 for L-652, 1.0 for A-43, and 1.16 for A-6 and A-IV.

other polypeptides, in which $\tau T/\eta_0$ increase remarkably with f_N[12,14,15,26] and depend less pronouncedly on molecular weight.[14,15,26]

B. Data in Mixed Solvents. ORD data taken in mixtures of *m*-cresol and EDC indicated that PCBL assumes an essentially helical conformation in these mixed solvents. It is therefore interesting to compare the dielectric behavior of PCBL in them with that in pure *m*-cresol at high temperatures. Both in *m*-cresol and in the mixed solvents, dielectric dispersion followed Cole–Cole plots. The numerical results derived therefrom are summarized in Table II. Examination with sample M-2 revealed no composition dependence of the dielectric behavior except near pure components.

The data for $\langle\mu^2\rangle^{1/2}$ and $\tau T/\eta_0$ in *m*-cresol at higher temperatures are in substantial accord with those in the mixed solvents. Figure 10 displays a double logarithmic plot of $\tau T/\eta_0$ vs. $\bar{N}_w$; here the data of Matsumoto et al.[20] for PBLG in helicogenic solvents are included for comparison. The data for PCBL show a feature characteristic of rodlike molecules, which fact conforms to the finding from the ORD data that PCBL is essentially helical under the same solvent conditions. The downward deviation of the data points for higher molecular weight samples (L-652 and L-651) may be an indication of chain flexibility expected for such high molecular weight samples. In this connection, we refer to the previous light scattering evidence that PCBL in helicogenic solvents is quite flexible.[1,27]

Precisely speaking, the f_N values determined from the Moffitt–Yang parameter b_0 suggest that the helix formation is still incomplete in the mixed solvents. The $\langle\mu^2\rangle^{1/2}$ of M-1 and M-2 in these solvents, when corrected for this effect, give 5.8 D for the monomeric dipole moment in the helical conformation.

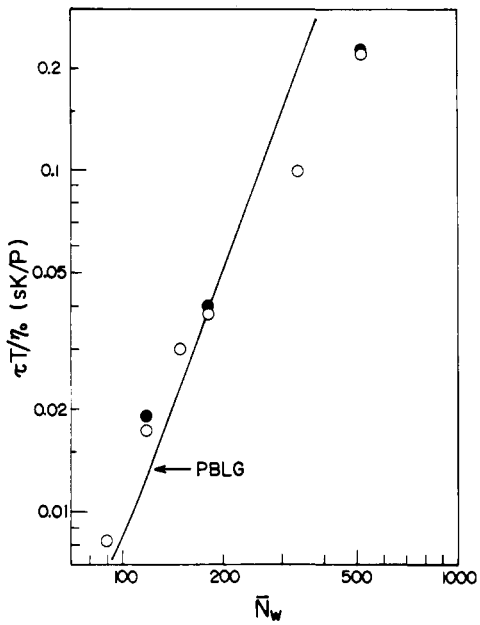

Figure 10. Double logarithmic plot of $\tau T/\eta_0$ vs. $\bar{N}_w$ for PCBL under the helicogenic conditions examined: ○, data in *m*-cresol; ●, data in EDC–*m*-cresol mixtures. The solid line represents the data of Matsumoto et al.[20] for PBLG in helicogenic solvents.

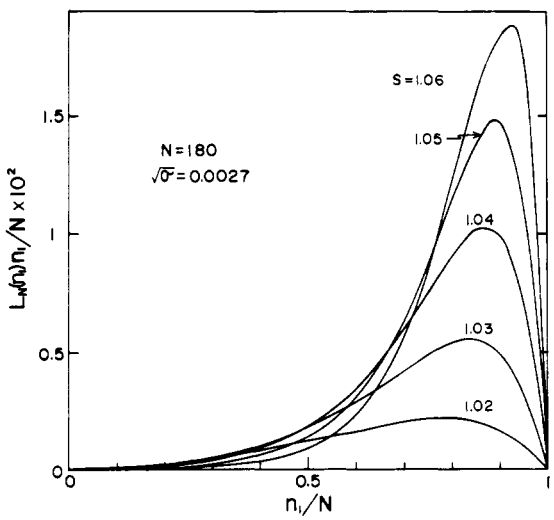

Figure 11. Weight distribution of helix lengths $L_N(n_1)n_1/N$ for N = 180 and the s values indicated. The helical fractions are 0.800 for s = 1.06, 0.732 for s = 1.05, 0.603 for s = 1.04, 0.396 for s = 1.03, and 0.197 for s = 1.02, respectively.

III. Discussion

A. Molecular Weight Heterogeneity. As has been noted in our previous paper,[20] the Cole–Cole plot for a helical polypeptide is sensitive to molecular weight heterogeneity. Cole and Cole[28] have suggested that the sector angle $\pi(1 - \alpha)$ of the arc may be used as a quantitative measure of it. Thus, according to the values of α listed in Table II, the molecular weight distributions of M-1, M-2, and M-4 are relatively narrow, while those of M-3, L-652, and L-651 are broad. None of these PCBL samples are as monodisperse as PBLG A-43 studied previously.[20] A broad molecular weight distribution of M-3 is consistent with its transition curve shown in Figure 1, which crosses those of other samples.

B. Average Conformation of a Polypeptide with Very Small σ. In order to know the conformation of a polypeptide with very small σ, we have examined the number of helical sections consisting of n_1 peptide residues, $L_N(n_1)$, and the average number of helical sections, g_N, in a polypeptide molecule as functions of N, s, and σ in the ranges of these parameters relevant to the PCBL–*m*-cresol system, using Nagai's theoretical expressions.[29,30] Figure 11 illustrates the weight distribution of helix lengths, $L_N(n_1)n_1/N$, as a function of reduced length n_1/N for $\sigma^{1/2}$ = 0.0027 and N = 180, with s as a parameter; the area under each curve is proportional to f_N. It is observed that each of the distribution curves has a sharp maximum at a value of n_1/N close to unity. Although not displayed here, the distribution is broader for larger σ and eventually becomes bimodal.[29] Figure 12 shows that if $\sigma^{1/2}$ is as small as 0.003 or less, g_N remains at unity near the helix side and then decreases to zero almost linearly with f_N. The initial horizontal part is suggestive of the chain unfolding which starts from chain ends and proceeds toward the central part of the chain. The subsequent decline in g_N is ascribed to the appearance of randomly coiled molecules in addition to the helical molecules flanked by two terminal random coil sections. In this situation, f_N should change in accordance with the change in population of these two types of molecules. Thus the transition should proceed approximately in all-or-none fashion at least for f_N greater than 0.2.

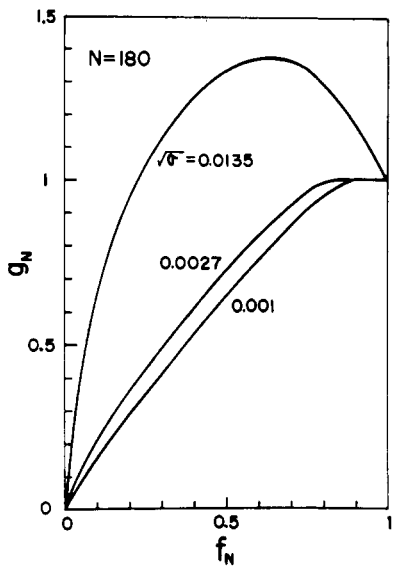

Figure 12. Average number of helical sequences in a polypeptide chain with N = 180 as a function of $\sigma^{1/2}$.

Equation 1 suggests that the static dielectric increment due to a helical section n_1 long is roughly proportional to n_1. Since only helical molecules make significant contributions to the dielectric dispersion (see Figure 5), this implies that the average dielectric behavior may be determined predominantly by longer helical sections and influenced little by the presence of shorter ones. From these considerations and the above theoretical consequence, the following dielectric behavior may be expected for a strongly cooperative system.

First, $\tau T/\eta_0$ may assume an essentially constant value characteristic of perfect helix over a substantial portion of the transition, i.e., for $f_N > 0.2$. The decline of $\tau T/\eta_0$ with increase in f_N as revealed in Figure 9 may be ascribed to several possibilities: (1) the motion of a helical section is hampered by the random coil sections flanked on its ends[12] and this effect may become more remarked as the random coil sections become longer, (2) the possible presence of

broken helices at large f_N, and (3) effects of molecular weight heterogeneity. The lowering of $\tau T/\eta_0$ at small f_N for higher molecular weight samples may reflect the contribution from random coil sections which has been neglected in the foregoing discussion.

Second, $\langle\mu^2\rangle^{1/2}$ should increase linearly with $f_N^{1/2}$. This prediction is consistent with the experimental results mentioned in A3 of the Results section. Detailed quantitative analysis of these results is made in the following subsection.

Third, it can be inferred from Figure 11 that the average length of helical sections in a helical molecule is rather closer to $Nf_N^{1/2}$. If this inference is correct, the partially helical molecule may behave dielectrically like an intact helix of $Nf_N^{1/2}$ in length. Our use of eq 2 in the analysis of dielectric data is then justified.

C. Analysis of $\langle\mu^2\rangle$ Data. The dipole moment of a linear chain molecule is a vector quantity analogous to the end-to-end vector of the molecule. Therefore, data for $\langle\mu^2\rangle$ of polypeptides may be treated by means of Nagai's theory of $\langle R^2\rangle$,[29] in which a real polypeptide chain is approximated by the following model: random coil sections are replaced by random flight chains with an effective dipole moment μ_c and helical sections consisting of n_1 peptide residues are replaced by rigid dipoles of magnitude $n_1\mu_h$ pointing to the helix axis; these are connected alternately by flexible joints. Nagai's expression of $\langle R^2\rangle$ for this model may be modified to give

$$\langle\mu^2\rangle = K_2\mu_c^2 + K_3\mu_h^2 \tag{4}$$

where K_2 and K_3 are known functions of N, s, and σ.[29,30] Equation 4 can be put in the form

$$K = \mu_c^2 + (K_3/K_2)\mu_h^2 \tag{5}$$

with

$$K = \langle\mu^2\rangle/K_2$$

and

$$K_2 = N(1 - f_N) \tag{6}$$

where N is the number of peptide residues in the polypeptide chain.

Thus data for $\langle\mu^2\rangle$ along with the thermodynamic data necessary to calculate K_2 and K_3 allow an experimental test of eq 5. If μ_c and μ_h are assumed to be constant in the transition region, a plot of K vs. K_3/K_2 should form a straight line, whose ordinate intercept and slope permit an experimental determination of μ_c and μ_h.

To do this test, $\sigma^{1/2}$ was assumed to be constant over the temperature range where the dielectric measurements were performed. First, f_N and K_3 were calculated for various values of $\sigma^{1/2}$ around 0.0027 as functions of s, and then K_3 values corresponding to the experimental f_N were interpolated. Then these values were used to compute the ratio K_3/K_2, while the values for K were obtained directly from the observed f_N and $\langle\mu^2\rangle$.

Figure 13 illustrates plots of K vs. K_3/K_2 constructed in this way for three PCBL samples ($\bar{N}_w$ = 180, 117, and 89). As predicted by eq 5 with constant μ_c and μ_h, the data points for different temperatures and molecular weights follow a straight line passing near the coordinate origin. From the slope of the straight line, μ_h is found to be 6.2 D, while μ_c is not obtained with any degree of certainty, because the intercept is too small; rough estimate indicates that μ_c does not exceed 10 D.

The solid lines in the top part of Figure 8 represent the theoretical values for $\langle\mu^2\rangle^{1/2}$ calculated with $\sigma^{1/2}$ = 0.0027 and the assumption that $\mu_c = \mu_h$ = 6.2 D, and agree closely with the experimental points over a substantial range of

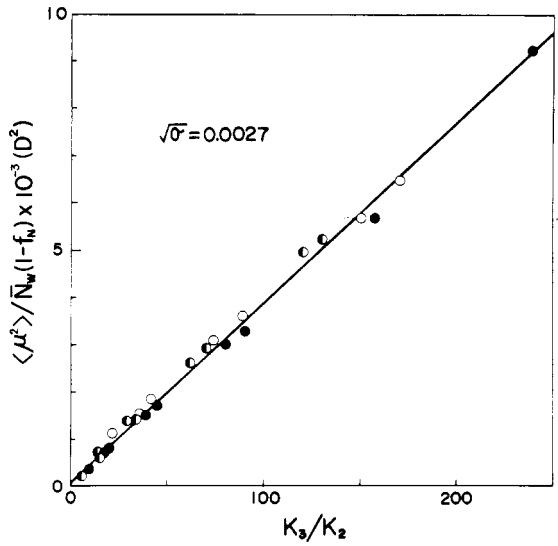

Figure 13. Plots of K vs. K_3/K_2 for PCBL in m-cresol according to eq 5: $\bar{N}_w$ = 180 (○), $\bar{N}_w$ = 117 (◐), and $\bar{N}_w$ = 89 (●). The straight line yields μ_h = 6.2 D (see text).

the transition. Similar analyses performed with the data for samples L-651 and L-652 ($\bar{N}_w$ = 551 and 332) yielded μ_h = 5.4 D. The bottom part of Figure 8 shows the agreement between theory and experiment for these two samples. The results obtained here should be compared with similar successes in interpreting light scattering data for partially helical polypeptides,[31,32] and have established experimentally the validity of the theories of molecular dimensions for polypeptides in the helix–coil transition region.[29,33,34]

Finally, a few comments on our analysis are necessary.

(1) The shape of our experimental $\langle\mu^2\rangle^{1/2}$ vs. f_N curves is convex upward and does not appear to vary sensitively with N. The theory predicts that it is also insensitive to the value of σ; the substantial portion of the curve around f_N = 0.5 maintains practically the same shape for $\sigma^{1/2}$ between 0.001 and 0.0075. Furthermore, the plot of K vs. K_3/K_2 was linear for any values of $\sigma^{1/2}$ within 0.001–0.0075, though the slope was larger for larger $\sigma^{1/2}$, but, for $\sigma^{1/2}$ above 0.005, the intercept gave unreasonably large values for μ_c. Thus the conclusion from our analysis is little affected, provided that $\sigma^{1/2}$ is in the range 0.001–0.005.

(2) At present we can give no reasonable explanation for the disparity between the derived μ_h values; 6.2 D for M-1, M-2, and M-4 and 5.4 D for L-651 and L-652. We will have to be satisfied with the fact that these values are consistent with that (5.8 D) derived from the measurements in helicogenic solvents. They are also comparable with the values (4–5 D) obtained for PBLG in helicogenic solvents.[20,35,36]

(3) In Figure 8, the theoretical $\langle\mu^2\rangle^{1/2} - f_N$ curves swing up in the region near the helix side, whereas the experimental data tend to level off at a lower value which is rather close to those obtained in helicogenic solvents (cf. Table II). This deviation from theory is indicative of flexibility of the PCBL helix in m-cresol at higher temperatures. Possible reasons for this are (1) inadequacy of the parameter values used in the present analyses, and (2) the presence of some molecular mechanisms other than those postulated in Nagai's theory, e.g., the real structure of polypeptide chains such as considered by Miller and Flory.[33]

(4) The magnitude of μ_c deserves our final comment. We quote a study of Wada et al.[12] who computed μ_c for poly-L-alanine to be $\mu_c = 0.825\mu_h$. This estimate is compatible with the present experimental results in which $\mu_h = 6 \pm 1$ D and $\mu_c = 6 \pm 3$ D.[37] However, Wada et al.[12] and Saruta et al.[26] observed relatively large dipolar contributions for

PBLA in the randomly coiled state. The data of Marchal et al.[15] for PBLG suggest that the μ_c values depend largely on solvent systems. Thus it is apparent that much remains to be elucidated on the dielectric properties of randomly coiled polypeptides in dilute solution.

IV. Conclusion

Dielectric dispersion measurements were made on PCBL in the helix–coil transition region, and mean-square dipole moments $\langle\mu^2\rangle$ and mean rotational relaxation times τ were obtained as functions of molecular weight and helical fraction. The experimental results and conclusions derived from their analyses in terms of statistical mechanical theories are summarized as follows.

(1) $\langle\mu^2\rangle^{1/2}$ increased rapidly with raising temperature, indicating that the average dimensions of PCBL largely increased on going from random coil to helix. The dependence of $\langle\mu^2\rangle^{1/2}$ on f_N was almost linear in $f_N^{1/2}$.

(2) The mean rotational relaxation time corrected for solvent viscosity and temperature, $\tau T/\eta_0$, changed only slightly with f_N except in the region of small f_N. Furthermore, $\tau T/\eta_0$ at fixed f_N showed molecular weight dependence characteristic of rodlike molecules. In both of these features, PCBL contrasts strikingly other polypeptides such as PBLA and PBLG.

(3) The features (1) and (2) can be explained if the transition is assumed to proceed almost in all-or-none fashion. This assumption is consistent with the previous finding from statistical thermodynamic analyses that the transition of PCBL in *m*-cresol is highly cooperative, with $\sigma^{1/2}$ being as small as 0.0025 or 0.0027. The difference in dielectric behavior in the transition region between PCBL and PBLA or PBLG is primarily ascribed to the large difference in their σ values.

(4) The data for $\langle\mu^2\rangle$ and f_N as functions of $\bar{N}_w$ conformed to Nagai's theory of $\langle R^2\rangle$ for interrupted helices, and yielded the result that the monomeric dipole moment μ_h in the helical conformation is 5.4–6.2 D, with $\sigma^{1/2}$ ranging from 0.001 to 0.005. These μ_h values are in good agreement with that obtained in helicogenic solvents and are also comparable with the values obtained previously for helical PBLG.

(5) From the present dielectric data as well as the previous light scattering data, it is now certain that PCBL in helicogenic solvents begins to exhibit flexibility at a relatively short chain length.

References and Notes

(1) M. Matsuoka, T. Norisuye, A. Teramoto, and H. Fujita, *Biopolymers*, **12**, 1515 (1973).
(2) (a) K. Nakamoto, H. Suga, S. Seki, A. Teramoto, T. Norisuye, and H. Fujita, *Macromolecules*, **7**, 784 (1974); (b) F. E. Karasz, J. M. O'Reilly, and H. E. Bair, *Biopolymers*, **3**, 241 (1965).
(3) B. H. Zimm, P. Doty, and K. Iso, *Proc. Natl. Acad. Sci. U.S.*, **45**, 1601 (1959).
(4) F. E. Karasz and J. M. O'Reilly, *Biopolymers*, **4**, 1015 (1966).
(5) T. Ackermann and E. Neumann, *Biopolymers*, **5**, 649 (1967).
(6) T. V. Barskaya, I. A. Bolotina, and O. B. Ptistyn, *Mol. Biol. (Moscow)*, **2**, 700 (1968).
(7) T. Norisuye, M. Matsuoka, A. Teramoto, and H. Fujita, *Polym. J.*, **1**, 691 (1970).
(8) N. Sayama, K. Kida, T. Norisuye, A. Teramoto, and H. Fujita, *Polym. J.*, **3**, 538 (1972).
(9) V. S. Ananthanarayanan, E. Leroy, and H. A. Scheraga, *Macromolecules*, **6**, 553 (1973).
(10) Y. Hayashi, A. Teramoto, K. Kawahara, and H. Fujita, *Biopolymers*, **8**, 403 (1969).
(11) F. Gaskin and J. T. Yang, *Biopolymers*, **10**, 631 (1971).
(12) A. Wada, T. Tanaka, and H. Kihara, *Biopolymers*, **11**, 587 (1972).
(13) E. Marchal, C. Dufour, and G. Spach, *J. Chim. Phys. Phys. Chim. Biol.*, **68**, 831 (1971).
(14) E. Marchal and C. Dufour, *J. Polym. Sci., Part C*, **30**, 77 (1970).
(15) E. Marchal, C. Dufour, and C. Strazielle, *Eur. Polym. J.*, **6**, 1147 (1970).
(16) C. Dufour and E. Marchal, *Biopolymers*, **11**, 1021 (1972).
(17) G. D. Fasman, M. Idelson, and E. R. Blout, *J. Am. Chem. Soc.*, **83**, 709 (1961).
(18) H. Fujita, "Foundations of Ultracentrifugal Analysis", Wiley, New York, N.Y., 1975.
(19) E. D. Washburn, Ed., "International Critical Tables", Vol. III, McGraw-Hill, New York, N.Y., 1928, p 29; Vol. VII, 1930, p 40; Beilstein, *Org. Chem.*, **6**, 345 (1956); **6**, 1287 (1966).
(20) T. Matsumoto, N. Nishioka, A. Teramoto, and H. Fujita, *Macromolecules*, **7**, 824 (1974).
(21) Measured $[m']_{436}$ values were converted to b_0 by using an empirically established $[m']_{436}$–f_N relation, from which f_N were calculated by $f_N = (182 - b_0)/712$.
(22) B. H. Zimm and J. K. Bragg, *J. Chem. Phys.*, **31**, 526 (1959).
(23) A. Wada, *J. Chem. Phys.*, **31**, 495 (1959).
(24) A. D. Buckingham, *Aust. J. Chem.*, **6**, 93, 323 (1952).
(25) J. Applequist and T. G. Mahr, *J. Am. Chem. Soc.*, **88**, 5419 (1966).
(26) S. Saruta, Y. Einaga, and A. Teramoto, unpublished data.
(27) J. Applequist and P. Doty, "Polyamino Acids, Polypeptides and Proteins", M. A. Stahmann, Ed., University of Wisconsin Press, Madison, Wis., 1962, p 161.
(28) K. S. Cole and R. H. Cole, *J. Chem. Phys.*, **9**, 341 (1941).
(29) K. Nagai, *J. Chem. Phys.*, **34**, 887 (1961).
(30) The Zimm–Bragg notations s and σ adopted in the present paper stand for σ and α^2 in Nagai's theory, respectively.
(31) K. Okita, A. Teramoto, and H. Fujita, *Polym. J.*, **1**, 582 (1970).
(32) T. Norisuye, A. Teramoto, and H. Fujita, *Polym. J.*, **4**, 323 (1973).
(33) W. G. Miller and P. J. Flory, *J. Mol. Biol.*, **15**, 298 (1966).
(34) M. Go, N. Saito, and M. Ochiai, *J. Phys. Soc. Jpn.*, **22**, 227 (1967).
(35) A. Wada, *Bull. Chem. Soc. Jpn.*, **33**, 822 (1960).
(36) E. H. Erenrich and H. A. Scheraga, *Macromolecules*, **5**, 746 (1972).
(37) This μ_c value is the average of those determined directly in *m*-cresol at 20° for M-2, M-3, M-4, and L-652.